Acta Cryst. (1979). A35, 665–672

An X-ray Diffraction Investigation of Chromium-Substituted Lithium Ferrite

BY R. W. CHEARY

The New South Wales Institute of Technology, PO Box 123, *Broadway, New South Wales, Australia* 2007

AND N. W. GRIMES

Physics Department, University of Aston, Birmingham B4 7ET, England

(*Received* 19 *July* 1978; *accepted* 23 *February* 1979)

Abstract

The loss of order in the lithium spinel system $Fe(Li_{0.5}Fe_{1.5-x/8}Cr_{x/8})O_4$ with $0 \le x \le 2$ is examined as a function of the Cr^{3+} ion concentration through an analysis of the X-ray superlattice line integrated intensities and line breadths. In these materials it is found that the growth of the antiphase domains is inhibited by the action of Cr^{3+} ions at the domain boundaries and it is shown that the observed variation of the long-range order parameter may be explained on the basis of a cation distribution on the octahedral sites which adheres to the so-called tetrahedral invariance condition. Furthermore, a correlation exists between the probability of an unstable Cr^{3+} ion configuration and the formation of domain boundaries. Some discussion is presented on the variation of the domain thickness distribution with Cr^{3+} ion content.

Introduction

Lithium spinels of the type $M^{3+}(Li_{0.5}M^{3+}_{1.5})O_4$, M corresponding to Fe, Al or Ga, possess an ordered structure on the octahedrally coordinated sites which is described by the cubic space group $P4_332$ or its enantiomorph $P4_132$ (Braun, 1952). The stability of the ordered arrangement arises principally because each Li^+ ion has only M^{3+} ions as nearest-neighbour octahedral ions. This configuration is referred to as tetrahedral charge invariance (Anderson, 1956) as it is equivalent to each tetrahedral group of octahedral ions comprising one Li^+ ion and three M^{3+} ions. For lithium ferrite this form of short-range order is rigidly adhered to in the disordered structure above 1008 K (Brunel & de Bergevin, 1966) and in the partially ordered structure immediately below this temperature (Cheary & Grimes, 1978).

When transition-metal ions with a large octahedral site stabilisation energy are substituted on the octahedral sites, the structure gradually reverts to the statistically face-centred form (space group $Fd3m$) normally associated with spinel compounds (Gorter, 1954; Blasse, 1964; Rogers, Germann & Arnott, 1965). This is indicated by the disappearance of the superlattice lines in the X-ray diffraction pattern. For Cr^{3+} or Rh^{3+} ions the critical concentration is approximately four substituted ions per unit cell, but with Mn^{3+} ions it is only two ions per unit cell. In these materials the site stabilization energy of the ions hinders the ordering process to the extent that at the critical concentration it is the dominant factor in determining the distribution of the transition-metal ions. On the basis of site stabilization energy alone the Mn^{3+} ion should be least effective in removing the order; however, being a Jahn–Teller ion it also creates localized distortions in the structure (Rogers, Germann & Arnott, 1965). The latter are made manifest through anomalies in the compositional dependence of the lattice parameter which arise, it is believed, from the formation of Mn^{3+} ion clusters. It is worth remarking that the squareness of the magnetic hysteresis loop in the system $Fe(Li_{0.5}Fe_{1.5-x/8}Mn_{x/8})O_4$ is optimized for substitutions x between two and three Mn^{3+} ions per unit cell.

In the present work the loss of order in the system $Fe(Li_{0.5}Fe_{1.5-x/8}Cr_{x/8})O_4$ is examined for substitutions of x ranging from zero to two Cr^{3+} ions per unit cell. This is done in terms of the compositional dependence of the lattice parameter, and the integrated intensities and profile breadths of the superlattice lines.

Experimental details and results

Seven specimens of composition $Fe(Li_{0.5}Fe_{1.5-x/8}Cr_{x/8})O_4$ were prepared under similar conditions for concentrations of 0, $\frac{1}{4}$, $\frac{1}{2}$, $\frac{3}{4}$, 1, $1\frac{1}{2}$ and 2 substituted Cr^{3+} ions per unit cell. This was done by the solid-state reaction of reagent grade Li_2CO_3 with the respective sesquioxides using a heat treatment procedure similar to that of Blasse (1964) and Rogers, Germann & Arnott (1965) and a cooling rate of approximately 20 K per hour from 1373 K. The X-ray diffraction patterns of

0567-7394/79/040665-08$01.00

the specimens indicated single-phase materials and all had features characteristic of the presence of antiphase domains, namely superlattice lines whose breadth increased with Cr^{3+} ion concentration and well resolved face-centred-cubic lattice lines.

The X-ray diffraction results for the present analysis were collected from a Philips powder diffractometer in its step-scanning mode with filtered Cr $K\alpha$ radiation and with the specimens held at room temperature (295 ± 3 K). Only the line profiles of the most intense superlattice lines not overlapping neighbouring lines (*i.e.* 110, 210, 211, 310 and 421) and the stronger lattice lines (*i.e.* 111, 220, 311, 400, 511/333, 440 and 533) were recorded. Bragg angles were estimated by the centroid method (Wilson, 1963*a*) and included corrections for the instrumental aberrations and the $K\alpha$ satellite lines (Cheary & Grimes, 1972). An extrapolation function of the form $\cos\theta\cot\theta$ was employed to determine the lattice parameters as this function most nearly produced linear plots. The centroid wavelength for Cr $K\alpha$ was taken to be 2·29095 Å, the weighted mean of the $K\alpha_1$ and $K\alpha_2$ wavelengths given in *International Tables for X-ray Crystallography* (1962).

Variance analysis (Wilson, 1962, 1963*a*,*b*) was used to evaluate the breadths of the line profiles. In this method the variance is calculated as a function of the range of integration 2σ about the centroid according to the relation,

$$W(2\sigma) = \int_{-\sigma}^{+\sigma} s^2 I(s)\,\mathrm{d}s \Big/ \int_{-\sigma}^{+\sigma} I(s)\,\mathrm{d}s, \qquad (1)$$

where $s = 2\sin\theta/\lambda - 1/d$.

When corrected for instrumental and physical aberrations, $W(2\sigma)$ approximates closely to a linear function of 2σ in the tails of the profile, *i.e.*

$$W(2\sigma) = -\frac{1}{2\pi^2}\frac{J'(0)}{J(0)}2\sigma - \frac{1}{4\pi^2}\left[\frac{J''(0)}{J(0)} + \left(\frac{K'(0)}{J(0)}\right)^2\right] + \frac{1}{\pi^4}\left(\frac{J'(0)}{J(0)}\right)^2, \qquad (2)$$

where $J(t) - jK(t)$ is defined as the mean value $\langle FF^* \rangle$ for cells separated by a distance t in the $[hkl]$ direction. In the present analysis the parameters $J'(0)/J(0)$ and $J''(0)/J(0)$ were estimated from the slopes and intercepts of the measured variance-range characteristics with the results from the fully ordered lithium ferrite specimen used to correct for effects of aberrations. It is worth remarking that the lattice lines from the chromium-substituted specimens were equally as sharp as those from the reference specimen, indicating that distortions in the structure do not contribute significantly to the broadening. Also, as the lattice parameter values estimated from the individual superlattice line positions did not deviate significantly from the main trend of the extrapolation plots, the centroid shift parameter $K'(0)/J(0)$ in the variance intercept term was assumed to be negligible. Further details of the correction procedures are given in Cheary & Grimes (1972, 1978).

Finally, the long-range order parameters S were obtained from the integrated intensities I_{hkl} of the superlattice lines relative to the 220 lattice line, *i.e.*

$$S^2 = \frac{(I_{hkl}/I_{220})x}{(I_{hkl}/I_{220})x=0}. \qquad (3)$$

This lattice line was chosen because of its independence of the state of order on the octahedral sites.

The experimental values for $J'(0)/J(0)$, $J''(0)/J(0)$, lattice parameter and long-range order parameter (weighted average for each specimen) are summarized in Table 1. In this table, the quoted experimental errors for the variance terms reflect the range of values for different background levels over which the variance-range graphs in the 'linear region' were indistinguishable from a straight line. For all of the profiles analysed, these errors were larger than those arising from counting statistics (Wilson, 1967). The experimental errors quoted for the lattice parameters indicate the range of values which give a reasonable fit to the extrapolation plots. On the other hand, those given for the long-range order parameters represent the scatter of values within each sample set.

Analysis and discussion of results

The integrated intensities and sharpness of the superlattice lines decrease rapidly with Cr^{3+} ion concentration indicating the presence of antiphase domains of decreasing size and substitutional disorder of the Cr^{3+} ions. As antiphase domains in unsubstituted lithium ferrite have a rapid rate of growth once the temperature drops below the transition value (Cheary & Grimes, 1978), the retention of these domains in the present substituted specimens, and not in the unsubstituted specimen, must be directly attributable to the Cr^{3+} ions. When spherically symmetric ions such as Ga^{3+} or Al^{3+} are substituted in lithium ferrite, long-range order is retained (Shulkes & Blasse, 1963) which suggests that the disorder in the Cr substituted compounds probably arises because of the large octahedral site stabilization energy of Cr^{3+} ions (McClure, 1957). This could act to reduce the mobility of the Cr^{3+} ions between octahedral sites relative to Fe^{3+} ions so that the domain growth rate, which is governed by the migration of the ions at the domain boundaries, is also reduced. This is illustrated in Fig. 1 for a possible (100) domain boundary. For the boundary to migrate to the new location by a diffusion process and yet satisfy the tetrahedral charge invariance condition, the Li^+ ions immediately to its left have to exchange position with

Table 1. *Experimental values of* $-J'(0)/J(0)$ ($\times 10^4$ Å^{-1}) *(upper value) and* $J''(0)/J(0)$ ($\times 10^6$ Å^{-2}) *(lower value) together with errors of measurement in parentheses, lattice parameter a, and long-range order parameter S as a function of x, the mean number of* Cr^{3+} *ions substituted per unit cell*

x	110	210	211	310	421	a (Å)	S
$\frac{1}{4}$	26 (7) 7 (2)	28 (5) 8 (2)	25 (7) 7 (2)	26 (12) 9 (11)	28 (11) 10 (5)	8·3320 (5)	0·98 (3)
$\frac{1}{2}$	67 (9) 67 (7)	69 (7) 53 (5)	63 (9) 52 (8)	64 (13) 52 (10)	67 (14) 72 (10)	8·3305 (5)	0·91 (5)
$\frac{3}{4}$	77 (12) 75 (9)	77 (10) 96 (8)	74 (12) 56 (9)	86 (23) 77 (19)	73 (28) 63 (19)	8·3295 (4)	0·85 (3)
1	119 (26) 198 (20)	102 (16) 144 (16)	118 (23) 173 (28)	104 (31) 121 (31)	139 (43) 203 (64)	8·3260 (5)	0·71 (4)
$1\frac{1}{2}$	136 (30) 206 (36)	142 (25) 219 (30)	132 (37) 199 (46)	– –	– –	8·3240 (5)	0·70 (4)
2	226 (21) 491 (40)	206 (20) 532 (42)	237 (29) 633 (64)	– –	– –	8·3205 (5)	0·68 (10)

3+ ions. When one or both of these ions have a low mobility (*i.e.* high activation energy) the probability of the boundary moving is small. If the 3+ ions involved in the corresponding exchange process on the right hand side of the boundary are also of the less mobile variety, the whole boundary will tend to be pinned down. Given that this type of behaviour applies to the present samples, it is probable that complete equilibrium was not achieved during preparation. This is supported by the observations of Rogers, Germann & Arnott (1965) who noted that for Mn^{3+} substituted lithium spinels prolonged annealing improved the resolution of the superlattice lines.

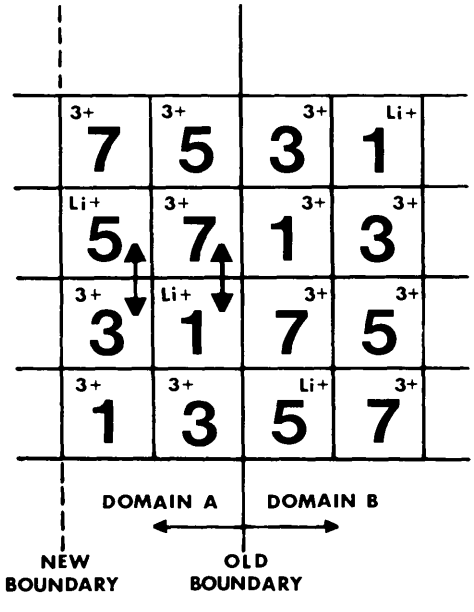

Fig. 1. (001) projection of the octahedral ion structure in the vicinity of a possible (100) antiphase domain boundary. The numbers within each square indicate the Z coordinates of these ions expressed in eighths of the unit-cell parameter for a boundary through the middle of the cell. The arrows indicate exchanges involved for boundary migration to the left.

Further evidence for the action of the Cr^{3+} ions at the domain boundaries is given by the variation of the experimental values for $J'(0)/J(0)$ with Cr^{3+} ion concentration. For a particular *hkl* line, $J'(0)/J(0)$ is determined by the mean thickness T of the antiphase domains in the [*hkl*] direction, and the types and abundance of allowed adjacent domains. In lithium ferrite, eight types of domain may form (Lefebvre, Portier & Fayard, 1974) as the octahedral ions can order in either a right-handed or left-handed form (*i.e.* space groups $P4_332$ or $P4_132$) with origins at any of the four equivalent face-centred positions. Given that each type of domain is equally abundant and all possible changes at the domain boundaries are equally likely,

$$\frac{J'(0)}{J(0)} = -\frac{8}{7T} \tag{4}$$

(Bessiere, Bley, Calvayrac, Lefebvre & Fayard, 1976). Due to the large experimental errors of the measurements, no significance can be attached to the variation of $J'(0)/J(0)$ with *hkl*, the line of diffraction, and so T was assumed to be independent of *hkl*. This is a justified approximation as the domain boundaries in unsubstituted lithium ferrite tend to form on {110} and, to a lesser extent, {100} planes (Cheary & Grimes, 1978), the net effect of which is only marginally different from the isotropic non-planar model. Actually, the conclusions drawn are not radically influenced by the boundary model adopted. This being so, the weighted mean value of $1/T$ was determined for each specimen and plotted as a function of x, the mean number of Cr^{3+} ions per unit cell (see Fig. 2).

The most striking feature of the graph in Fig. 2 is its linearity and to appreciate the significance of this it is necessary to examine the relationship between $1/T$ and the surface area at the domain boundaries. For T independent of *hkl*, the shape of the domain, on average, will be spherical with a mean diameter $D = 3T/2$. To a first approximation, this gives:

surface area per domain $= \pi D^2$,
number of domains per unit volume $= 6/\pi D^3$,

so that,

domain surface area per unit volume $= 3/D = 2/T$.

Fig. 2, therefore, shows that the total domain boundary area per unit volume of material increases uniformly and at a rate of $1{\cdot}9 \pm 0{\cdot}1$ Å^2/Å^3 for each added Cr^{3+} ion per unit cell. Clearly the Cr^{3+} ions play a direct part in determining the domain boundary area.

This behaviour could be explained by assuming that the Cr^{3+} ions segregate at the domain boundaries.

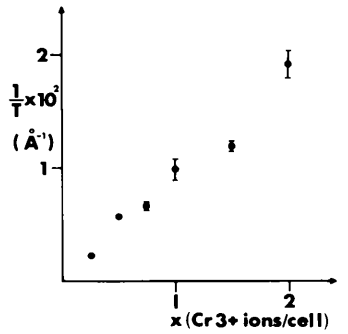

Fig. 2. Mean value of $1/T$ for each specimen, weighted according to the accuracy of each measurement of $J'(0)/J(0)$, as a function of x, the mean number of Cr^{3+} ions per unit cell. The error bars represent the scatter of values calculated within each specimen set.

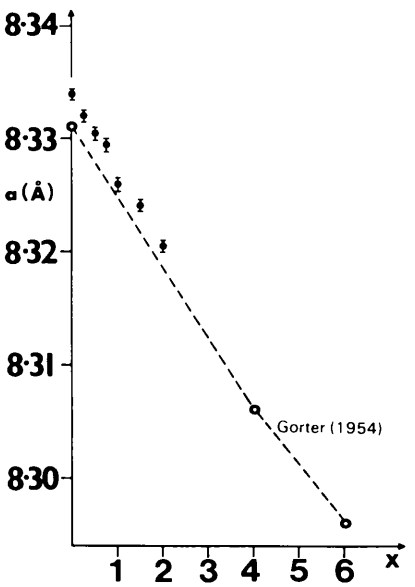

Fig. 3. Variation of lattice parameter a as a function of x, the mean number of Cr^{3+} ions per unit cell. Also included are values of a measured by Gorter (1954).

However, this is unlikely as the lattice parameter a varies almost linearly with x, the number of Cr^{3+} ions per unit cell, and has a slope da/dx almost identical to that obtained from Gorter (1954) for a wider range of concentrations as shown in Fig. 3. It is worth remarking that his absolute values of 'a' differ by a constant amount from the present measurements (*i.e.* approximately 0·0015 Å), but this is probably due to the different methods of determination. In addition, boundary segregation would not produce the rapid change of long-range order parameter observed as most of the structure within the domain would remain fully ordered and disorder would exist only at the boundaries. For the present specimens, therefore, the Cr^{3+} ions would appear to be homogeneously distributed throughout the structure.

The homogeneity assumption simplifies the calculation of the long-range order parameter because the integrated intensity I can then be approximated as

$$I = \langle FF^* \rangle \simeq \langle F \rangle \langle F^* \rangle, \tag{5}$$

where F is the structure factor and $\langle\ \rangle$ represents mean value. (Note: strictly speaking this approximation is only valid for uncorrelated random substitution, but as the present case seems unlikely to be radically different, it is probably justified.) For the superlattice lines the average structure factor $\langle F \rangle$ is given approximately by

$$\langle F \rangle = K(\langle f_d \rangle - \langle f_b \rangle), \tag{6}$$

where K is a constant and $\langle f_d \rangle$ and $\langle f_b \rangle$ refer to the average scattering factors on the d sites and b sites, respectively, of the space group $P4_332$ given in *International Tables for X-ray Crystallography* (1952). When $x = 0$, the d sites are occupied by Fe^{3+} ions and the b sites by Li^+ ions.

Suppose that when x Cr^{3+} ions are substituted per unit cell, the average distribution on the octahedral sites is η Cr^{3+} ions, ξ Fe^{3+} ions and $4 - (\eta + \xi)$ Li^+ ions on the $4b$ sites and $(x - \eta)$ Cr^{3+} ions, $(12 - x - \xi)$ Fe^{3+} and $(\xi + \eta)$ Li^+ ions on the $12d$ sites. It is assumed here that no Li^+ ions enter the tetrahedral sites of the structure for $x \leq 2$ as indicated by Gorter (1954). The average structure factor $\langle F \rangle$ will be given by,

$$\langle F \rangle = K\frac{x - 4\eta}{12} f_{Cr^{3+}} + \left(\frac{12 - x - 4\xi}{12}\right) f_{Fe^{3+}} - \left(\frac{12 - 4\xi - 4\eta}{12}\right) f_{Li^+}$$

and to a first approximation

$$f_{Cr^{3+}} \simeq f_{Fe^{3+}} \simeq \frac{(f_{Fe^{3+}} + f_{Cr^{3+}})}{2} = f_{3+},$$

so that

$$\langle F \rangle \simeq K[1 - (\xi + \eta)/3](f_{3+} - f_{\mathrm{Li}^+}) \quad (7)$$

and the long-range order parameter S will be given by

$$S = 1 - (\xi + \eta)/3$$

$$= 1 - \text{mean no. of } \mathrm{Li}^+ \text{ displaced from } b \text{ sites}/3. \quad (8)$$

Alternatively, if α is the fraction of 3+ ions on the b sites relative to the mean number of Cr^{3+} ions per unit cell [*i.e.* $\alpha = (\xi + \eta)/x$], then

$$S = 1 - \alpha x/3. \quad (9)$$

The experimental values for S given in Fig. 4 vary almost linearly with x indicating that α is a constant which in this instance is $0{\cdot}7 \pm 0{\cdot}1$. On average therefore, the number of Li^+ ions displaced from the b sites will be approximately 70% of the number of Cr^{3+} ions in the unit cell. If the Cr^{3+} ions within the domains were randomly distributed on the octahedral sites $\frac{2}{3}$ would occupy d sites and $\frac{1}{3}$ would occupy b sites giving a value for $\alpha = \frac{1}{3}$ and a variation in S as shown in Fig. 4(*a*).

The poor agreement of the random model is not surprising as it makes no allowance for the fact that perfect short-range order should be maintained on the octahedral sites (*i.e.* the tetrahedral invariance condition) or that long-range ordering forces are present. Unlike Al^{3+} or Fe^{3+} ions, Cr^{3+} ions are less susceptible to long-range ordering because of their site stabilization energies. Thus, we can assume that they may enter b sites without necessarily being dislodged provided that the stronger condition of tetrahedral invariance is not violated.

To develop this further it is necessary to refer to the structure given in projected form in Fig. 5(*a*) in terms of the location of Li^+ ions (on b sites) for one of the eight possible types of ordered structure. When Cr^{3+} ions occupy d sites the structure remains fully ordered. If, on the other hand, one occupies a b site, such as position 5 in Fig. 5(*a*), the Li^+ ions normally associated with this position and the neighbouring position 1 must occupy adjacent d sites, as illustrated in Fig. 5(*b*), for tetrahedral invariance to be maintained. The same applies if a Cr^{3+} ion occupies position 1. A readjustment must also occur if Cr^{3+} ions occupy either of the other pair of b sites (see Fig. 5*c*). If the Li^+ ions occupy locations other than those indicated or if Cr^{3+} ions occupy the alternative d sites as well as the corresponding b sites, the tetrahedral charge-invariance principle will be violated and the structure will tend to be unstable.

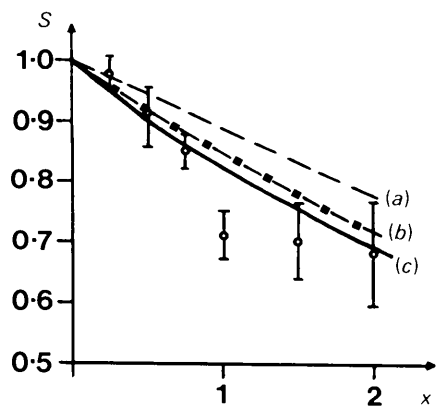

Fig. 4. Variation of experimental values for long-range order parameter S as a function of x, the mean Cr^{3+} ion concentration per unit cell, compared with the following theoretical models: (*a*) random substitution of the Cr^{3+} ions on the octahedral sites, (*b*) random substitution of Cr^{3+} ions on the octahedral sites with the constraint of tetrahedral charge invariance, (*c*) model (*b*) including the effect of disorder at the domain boundaries.

In the analysis that follows, the b sites are considered in pairs (*i.e.* positions 1 and 5, and positions 7 and 3 in Fig. 5*a*) and the alternative d sites associated with each of them are referred to as either stable or unstable d sites. When a Cr^{3+} ion occupies a b site, the alternative d sites become unstable to Cr^{3+} ion occupation. These are termed stable d sites when the neighbouring b sites are free of Cr^{3+} ions. The eight d sites which do not act as alternative sites for the Li^+ ions will always be stable. With this nomenclature it is possible to express all the possible Cr^{3+} ion configurations in a relatively simple manner. This is shown in Table 2 which also gives the random probability of each particular configuration for unit cells containing up to four Cr^{3+} ions per unit cell.

Table 2 allows the conditional probability $Q(n/m)$ of n Li^+ ions being displaced from b sites to be determined given that the particular cell structure does not violate the tetrahedral invariance condition and contains m Cr^{3+} ions. The expected number of Li^+ ions displaced per unit cell $E(x)$ for an average concentration of x Cr^{3+} ions per unit cell will, therefore, be given by

$$E(x) = \sum_m P(m/x)\left(\sum_{n=0,2,4} nQ(n/m)\right), \quad (10)$$

where $P(m/x)$ is the conditional probability of a cell comprising m Cr^{3+} ions given that x is average concentration. If it is assumed that the probability of

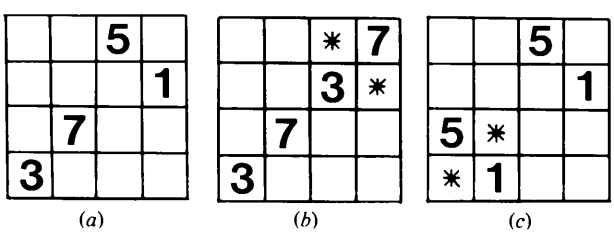

Fig. 5. (*a*) Li^+ ion configuration in projected form of octahedral ion structure for one type of domain, (*b*) and (*c*) alternative Li^+ ion configurations when Cr^{3+} ions occupy any of the normal Li^+ ion positions denoted by *.

any d site in the structure being occupied by a Cr^{3+} ion is $x/12$ and by an Fe^{3+} ion is $(1 - x/12)$, the probability $P(m/x)$ will be given by the binomial distribution

$$P(m/x) = \frac{12!}{(12-m)!m!}\left(\frac{x}{12}\right)^m\left(1-\frac{x}{12}\right)^{12-m}. \quad (11)$$

Values for $Q(n/m)$ for m up to $6Cr^{3+}$ ions per cell are given in Table 3 along with the expected number of Li^+ ions displaced.

The variation of long-range order parameter S given by $1 - E(x)/3$, as shown in Fig. 4(b), is clearly an improvement on the earlier model. Nevertheless, even better agreement can be obtained by including the influence of the domain boundaries. An approximate method of doing this is to assume that cells through which domain boundaries pass behave as disordered cells and do not contribute to the superlattice line intensities (*i.e.* $\langle F \rangle = 0$). The fraction of this type can be estimated from the mean domain thickness T. In a unit length along the [100] direction there are $1/a$ unit cells and $1/T$ domain boundaries. Therefore, the fraction of cells containing boundaries will be approximately a/T. However, even for the simplest situation of (100) boundaries there are four possible boundary locations in the spinel structure; three within the cell structure and one on the cell face. Consequently, the fraction of cell contributing to the superlattice line intensity will be $(1 - 3a/4T)$ giving a variation of S of the form

$$S = (1 - 3a/4T)^{1/2}S_0, \quad (12)$$

where S_0 is the long-range order parameter given by the substitutional model. The influence of disordered boundary cells on the tetrahedral invariance model is given in Fig. 4(c). The agreement with experiment is within the bounds of the experimental errors.

Table 2. *Possible* Cr^{3+} *configurations on the octahedral sites along with their associated probabilities and number of* Li^+ *ions displaced for up to four* Cr^{3+} *ions per unit cell*

The symbols used to describe the configurations are as follows; d = d site, b = b site, Sd = stable d site, Ud = unstable d site, sm b = same pair of b sites, and opp$b$ = opposite pair of b sites. Example; 2 opp$b$, 1Sd is to be interpreted as 1 Cr^{3+} ion on each pair of b sites and 1 Cr^{3+} ion on a stable d site.

Cr^{3+} ions per cell	Total no. of config'ns	Cr^{3+} ion config'n	No. of equiv. config'ns	Prob. of config'n	No. of Li^+ disp.
(a) Stable configurations					
1	16	1d	12	3/4	0
		1b	4	1/4	2
2	$\frac{16!}{14!\,2!}$	2d	12 × 11/2!	66/120	0
		1b, 1Sd	10 × 4	40/120	2
		2sm$b$	4 × 1/2!	2/120	2
		2 opp$b$	4 × 2/2!	4/120	4
3	$\frac{16!}{13!\,3!}$	3d	12 × 11 × 10/3!	220/560	0
		1b, 2Sd	10 × 9 × 4/2!	180/560	2
		2sm$b$, 1Sd	10 × 4 × 1/2!	20/560	2
		2opp$b$, 1Sd	8 × 4 × 2/2!	32/560	4
		3b	4 × 3 × 2/3!	4/560	4
4	$\frac{16!}{12!\,4!}$	4d	12 × 11 × 10 × 9/4!	495/1820	0
		1b, 3Sd	10 × 9 × 8 × 4/3!	480/1820	2
		2sm$b$, 2Sd	10 × 9 × 4 × 1/2!2!	90/1820	2
		2opp$b$, 2Sd	8 × 7 × 4 × 2/2!2!	112/1820	4
		3b, 1Sd	4 × 3 × 2 × 8/3!	32/1820	4
		4b	1	1/1820	4
(b) Unstable configurations					
2	$\frac{16!}{14!\,2!}$	1b, 1Ud	4 × 2	8/120	
3	$\frac{16!}{13!\,3!}$	1b, 1Sd, 1Ud	10 × 4 × 2	80/560	
		2opp$b$, 1Ud	4 × 2 × 4/2!	16/560	
		1b, 2Ud	4 × 2 × 1/2!	4/560	
		2sm$b$, 1Ud	4 × 1 × 2/2!	4/560	
4	$\frac{16!}{12!\,4!}$	1b, 2Sd, 1Ud	10 × 9 × 2 × 4/2!	360/1820	
		1b, 1Sd, 2Ud	10 × 2 × 1 × 4/2!	40/1820	
		2sm$b$, 1Sd, 1Ud	4 × 1 × 10 × 2/2!	40/1820	
		2sm$b$, 2Ud	4 × 1 × 2 × 1/2!2!	2/1820	
		2opp$b$, 1Sd, 1Ud	8 × 4 × 4 × 2/2!	128/1820	
		2opp$b$, 2Ud	4 × 3 × 4 × 2/2!2!	24/1820	
		3b, 1Ud	4 × 3 × 2 × 4/3!	16/1820	

In the context of the calculated probabilities it is worth remarking that domain boundaries could nucleate from unstable Cr^{3+} ion configurations. For these, stability can be achieved in two stages:

(i) by the relocation of Li^+ ions to form a domain boundary within one cell;

(ii) by cooperative readjustment of Li^+ ions in neighbouring cells, next-nearest neighbour cells and so on, to regain tetrahedral invariance stability, leading eventually to a domain boundary limited in size only by the proximity of other boundaries.

Unfortunately, it is not a simple matter to calculate the outcome of this behaviour. It is interesting to note, however, that the probability $P_u(x)$ of an unstable cell for a Cr^{3+} ion concentration x, as given by

$$P_u(x) = \sum_m R_u(m) P(m/x), \qquad (13)$$

where $R_u(m)$ is the probability of an unstable cell when it contains m Cr^{3+} ions (obtained from Table 2), is inversely proportional to the mean area per domain A, given by πD^2 ($\simeq \pi 9T^2/4$), as shown in Fig. 6.

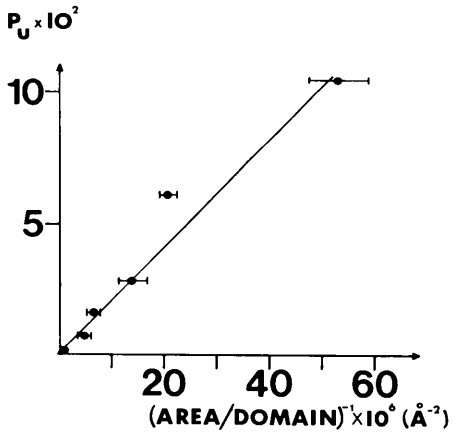

Fig. 6. Plot of the calculated probability of an unstable cell $P_u(x)$ as a function of A^{-1} where A is the mean surface area per domain in Å^2 given by $9\pi T^2/4$. The error bars represent the scatter of values calculated within each specimen set.

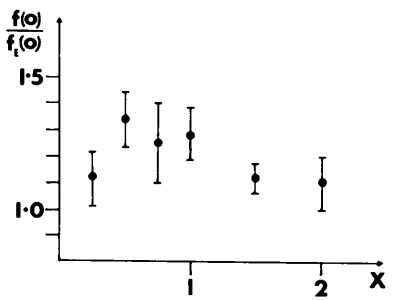

Fig. 7. Experimental variation of $f(0)/f_E(0)$ with x, the mean number of Cr^{3+} ions per unit cell along with the experimental errors calculated from the scatter of values within each specimen set.

Table 3. *Values for the conditional probability $Q(n/m)$, where n is the number of Li^+ ions displaced with m Cr^{3+} ions present in the unit cell, and the expected number of Li^+ ions displaced from b sites, $E(x)$, as a function of x, the mean Cr^{3+} ion concentration per unit cell*

	Number of Cr^{3+} ions/cell m					
n	1	2	3	4	5	6
0	0·75	0·59	0·48	0·41	0·36	0·32
2	0·25	0·38	0·44	0·47	0·49	0·50
4	0	0·04	0·08	0·12	0·16	0·18
x	$\frac{1}{4}$	$\frac{1}{2}$	$\frac{1}{4}$	1	$1\frac{1}{2}$	2
$E(x)$	0·12	0·24	0·35	0·45	0·65	0·82

Finally, it is worth commenting on the values for $J''(0)/J(0)$ given by the variance analysis. For an antiphase domain structure this parameter is given by (Wilson, 1963*b*)

$$\frac{J''(0)}{J(0)} = \left(\frac{J'(0)}{J(0)}\right)^2 f(0)T,$$

where $f(0)$ is the value of the domain thickness distribution $f(y)$ at $y = 0$. When the probability of a change per unit length from one domain to the next is independent of the size of the domain, $f(y)$ is given by the exponential distribution (Wilson, 1943)

$$f_E(y) = \frac{1}{T}\exp(-y/T),$$

so that

$$\frac{J''(0)}{J(0)} = \left[\frac{J'(0)}{J(0)}\right]^2 \frac{f(0)}{f_E(0)}. \qquad (14)$$

The mean values of $f(0)/f_E(0)$ for each specimen estimated from the experimental values of $J'(0)/J(0)$ and $J''(0)/J(0)$ and weighted according to the accuracy of each result, is plotted in Fig. 7 as a function of x.

It is clear from these results that the domain thickness distribution does not change significantly with Cr^{3+} ion concentration. On the basis of previous interpretations of $f(0)/f_E(0)$ (Cheary & Grimes, 1978) the domain structure comprises a very large number of small domains interspersed with a small number of large domains, a situation not unlike that associated with discontinuous grain growth.

References

ANDERSON, P. W. (1956). *Phys. Rev.* **102**, 1008–1013.
BESSIERE, M., BLEY, M., CALVAYRAC, Y., LEFEBVRE, S. & FAYARD, M. (1976). *J. Appl. Cryst.* **9**, 353–354.
BLASSE, G. (1964). *Philips Res. Rep. Suppl.* 3.
BRAUN, P. B. (1952). *Nature (London)*, **170**, 1123.

BRUNEL, M. & DE BERGEVIN, F. (1966). *Solid State Commun.* **4**, 165–168.
CHEARY, R. W. & GRIMES, N. W. (1972). *J. Appl. Cryst.* **5**, 57–63.
CHEARY, R. W. & GRIMES, N. W. (1978). *Acta Cryst.* A**34**, 74–84.
GORTER, E. W. (1954). *Philips Res. Rep.* **9**, 403–423.
International Tables for X-ray Crystallography (1952). Vol. I. Birmingham: Kynoch Press.
International Tables for X-ray Crystallography (1962). Vol. III. Birmingham: Kynoch Press.
LEFEBVRE, S., PORTIER, R. & FAYARD, M. (1974). *Phys. Status Solidi A*, **24**, 79–89.
MCCLURE, D. S. (1957). *J. Phys. Chem. Solids*, **3**, 311–316.
ROGERS, D. B., GERMANN, R. W. & ARNOTT, R. J. (1965). *J. Appl. Phys.* **36**, 2338–2342.
SHULKES, J. A. & BLASSE, G. (1963). *J. Phys. Chem. Solids*, **24**, 1651–1655.
WILSON, A. J. C. (1943). *Proc. R. Soc. London Ser. A*, **181**, 360–368.
WILSON, A. J. C. (1962). *Proc. Phys. Soc.* **80**, 286–294.
WILSON, A. J. C. (1963*a*). *Mathematical Theory of X-ray Powder Diffractometry*. Eindhoven: Centrex.
WILSON, A. J. C. (1963*b*). *Proc. Phys. Soc.* **81**, 41–46.
WILSON, A. J. C. (1967). *Acta Cryst.* **23**, 888–898.

Acta Cryst. (1979). A**35**, 672–675

Overall Values of Conventional Discrepancy Indices in the Presence of Random Positional Errors: Crystal with Similar Atoms

BY S. PARTHASARATHY AND M. N. PONNUSWAMY

Department of Crystallography and Biophysics, University of Madras, Guindy Campus, Madras* 600 025, *India*

(*Received* 9 *January* 1979; *accepted* 19 *March* 1979)

Abstract

The overall values of the conventional discrepancy indices based on structure amplitudes [*i.e.* $R(F)$] and intensities [*i.e.* $R(I)$] are evaluated as functions of the mean positional error $\langle|\Delta\mathbf{r}|\rangle$ and the fractional contribution of the known atoms to the local mean intensity (*i.e.* σ_1^2) for crystals containing a large number of similar atoms. The results are tabulated for both the centrosymmetric and non-centrosymmetric cases.

1. Introduction

The use of discrepancy indices in the various stages of crystal structure analysis is well known. Of the various indices that have been proposed (Srinivasan & Parthasarathy, 1976; hereafter SP, 1976), the conventional discrepancy indices [denoted by $R(F)$ and $R(I)$] are the ones normally computed in crystallographic programs. Wilson (1950) worked out the maximum probable values of $R(F)$ for centrosymmetric and non-centrosymmetric (hereafter *C* and *NC*) cases when the trial structure is of the unrelated *complete* (*i.e.* $\sigma_1^2 = 1$)† type. He also considered the effect of a single badly misplaced atom on $R(F)$ and $R(I)$ when the trial structure is of the complete type (Wilson, 1969). Luzzati (1952) considered the effect of random positional errors on $R(F)$ and obtained $R(F)$ as a function of $\sin\theta$ for different fixed values of the mean positional error $\langle|\Delta\mathbf{r}|\rangle$. His results, however, apply only for a complete model (*i.e.* $\sigma_1^2 = 1$). Srinivasan, Raghupathy Sarma & Ramachandran (1963) worked out the values of $R(F)$ for two limiting situations, namely, the related (*i.e.* $\langle|\Delta\mathbf{r}|\rangle = 0$) and the unrelated (*i.e.* $\langle|\Delta\mathbf{r}|\rangle$ very large) cases and their results apply to a complete as well as an incomplete type of trial structure (*i.e.* $0 < \sigma_1^2 \leq 1$). Thus the *overall values* of $R(F)$ and $R(I)$ [denoted by $\bar{R}(F)$ and $\bar{R}(I)$, respectively] applicable for the general case of an *imperfectly related* (*i.e.* $\langle|\Delta\mathbf{r}|\rangle$ finite) *incomplete* (*i.e.* $0 < \sigma_1^2 \leq 1$) type are not available. These overall values are important because: (1) crystallographers judge the correctness of trial structures generally from the overall values of the conventional R indices computed with all the observed independent reflections as a single group; (2) the trial structures met with in practice are such that they often account for only part of the structure (*i.e.* $\sigma_1^2 < 1$) and, further, they involve atoms with random positional errors. In the presence of random positional errors the R indices are expected to be monotonically increasing functions of $(\sin\theta)/\lambda$ (hereafter S). In this paper we shall therefore obtain the theoretical overall values of $R(F)$ and $R(I)$ as functions of σ_1^2 and $\langle|\Delta\mathbf{r}|\rangle$ for the general case of an imperfectly related incomplete model. The results obtained here are applicable only for crystals containing similar atoms.

* Contribution No. 485.
† See § 2 for a definition of σ_1^2.

0567-7394/79/040672-04$01.00